








Quasars: Standard Candles up to $z = 7.5$ with the Precision of Supernovae Ia

M. G. Dainotti^{1,2,3,11} , G. Bargiacchi^{4,5} , A. Ł. Lenart⁶ , S. Nagataki^{7,8,9} , and S. Capozziello^{4,5,10} ¹ National Astronomical Observatory of Japan, 2 Chome-21-1 Osawa, Mitaka, Tokyo 181-8588, Japan; maria.dainotti@nao.ac.jp, mariagiovannadainotti@yahoo.it² The Graduate University for Advanced Studies, SOKENDAI, Shonankokusaimura, Hayama, Miura District, Kanagawa 240-0193, Japan³ Space Science Institute, 4765 Walnut St, Suite B, Boulder, 80301 CO, USA⁴ Scuola Superiore Meridionale, Largo S. Marcellino 10, I-80138 Napoli, Italy⁵ Istituto Nazionale di Fisica Nucleare (INFN), Sez. di Napoli, Complesso Univ. Monte S. Angelo, Via Cinthia 9, I-80126 Napoli, Italy⁶ Astronomical Observatory, Jagiellonian University, ul. Orła 171, 31-501 Kraków, Poland⁷ Interdisciplinary Theoretical & Mathematical Science Program, RIKEN (iTHEMS), 2-1 Hirosawa, Wako, Saitama 351-0198, Japan⁸ RIKEN Cluster for Pioneering Research, Astrophysical Big Bang Laboratory (ABBL), 2-1 Hirosawa, Wako, Saitama 351-0198, Japan⁹ Astrophysical Big Bang Group (ABBG), Okinawa Institute of Science and Technology Graduate University (OIST), 1919-1 Tancha, Okinawa 904-0495, Japan¹⁰ Dipartimento di Fisica “E. Pancini”, Università degli Studi di Napoli Federico II, Complesso Univ. Monte S. Angelo, Via Cinthia 9, I-80126 Napoli, Italy; maria.dainotti@nao.ac.jp

Received 2023 February 25; revised 2023 April 4; accepted 2023 April 18; published 2023 June 9

Abstract

Currently, the Λ cold dark matter model, which relies on the existence of cold dark matter and a cosmological constant Λ , best describes the universe. However, we lack information in the high-redshift (z) region between Type Ia supernovae (SNe Ia; up to $z = 2.26$) and the cosmic microwave background ($z = 1100$), an interval crucial to test cosmological models and their possible evolution. We have defined a sample of 983 quasars up to $z = 7.54$ with a reduced intrinsic dispersion $\delta = 0.007$, which determines the matter density parameter Ω_M with the same precision of SNe Ia. Although previous analysis have used quasars as cosmological tools, this is the first time that high-redshift sources, in this case quasars, as standalone cosmological probes yield such tight constraints on Ω_M . Our results show the importance of correcting cosmological relationships for selection biases and redshift evolution and how the choice of a golden sample reduces considerably the intrinsic scatter. This proves the reliability of quasars as standard cosmological candles.

Unified Astronomy Thesaurus concepts: [quasars \(1319\)](#)

1. Introduction

Nowadays it is time for the scavenger hunt for cosmological parameters such as the Hubble constant, H_0 , and the matter density parameter, Ω_M . The main challenge is to cast light further on which is the most suitable description of the universe. Currently, the most accredited model is the Λ CDM model, which includes a cold dark matter (CDM) component and a dark energy associated with a cosmological constant Λ , as suggested by the current accelerated expansion of the universe (Riess et al. 1998; Perlmutter et al. 1999). Predictions from this scenario are compatible with observational probes such as the cosmic microwave background (CMB; Planck Collaboration et al. 2020) at redshift $z = 1100$, baryon acoustic oscillations (Alam et al. 2021), and Type Ia supernovae (SNe Ia) observed at low z up to $z = 2.26$ (Rodney et al. 2015). However, we lack information on intermediate redshifts between SNe Ia and the CMB. Having reliable cosmological candles at intermediate redshifts between SNe Ia and the CMB could be the crucial turning point to understanding to what extent the current cosmological Λ CDM model is the most suitable one. To this end, the community strives to reduce as much as possible the uncertainties on cosmological parameters and to find probes at intermediate redshifts which can be considered standard candles (Yonetoku et al. 2004). Given the

current interest of the community in quasars as reliable cosmological tools (Risaliti & Lusso 2019; Dainotti et al. 2022a; Bargiacchi et al. 2022; Khadka et al. 2023; Lenart et al. 2023), we focus on the hunt for a gold sample for quasars, as already done for gamma-ray bursts (GRBs; Dainotti et al. 2010, 2013, 2015, 2016, 2020, 2021b, 2022b, 2022c, 2022d, 2023b). We propose an approach to the use of quasars as standard candles similar to the one done for SNe Ia 25 yr ago, but quasars are observed at much larger distances (up to $z = 7.54$). To tackle such an approach we need a standardizable candle and in this regard, a relation exists between the X-ray and the ultraviolet (UV) luminosities of quasars (known as the Risaliti–Lusso relation, hereafter called the RL relation). To use this, quasar emission mechanisms need to be very well understood and the relation at play should not be affected by redshift evolution (a change in redshift) and selection biases. Namely, such a relation should remain the same at all redshifts, or if there is a redshift evolution this should be properly accounted for before its use as a cosmological tool. Dainotti et al. (2022a) have already demonstrated that the RL relation is not induced by selection biases or redshift evolution, but it is intrinsic to the physics of quasars. Here we have presented two main gold samples of quasars. One is built from a flat Λ CDM model with $\Omega_M = 0.3$ and $H_0 = 70 \text{ km s}^{-1} \text{ Mpc}^{-1}$ and is composed of 983 quasars up to $z = 7.54$, which constrains the parameter Ω_M in the assumed cosmology with the same precision as SNe Ia in the Pantheon sample. The other one is instead obtained through a circularity-free procedure and consists of 975 sources with the same maximum redshift of $z = 7.54$. The paper is structured in data and methodology, Section 2, where we detail the samples, and all methods and results, Sections 3 and 4, where the choice of the golden sample assuming a given cosmology is explained and the

¹¹ First and second authors share the same contribution.

solution for a golden sample completely independent from the circularity problem including the Markov Chain sampling uncertainty results is presented. We discuss our findings in Section 5.

2. Data Set and Methodology

Our initial quasar sample is the most recent one released for cosmological studies (Lusso et al. 2020). It consists of 2421 sources in the redshift range between $z = 0.009$ and $z = 7.54$ (Bañados et al. 2018) collected from eight catalogs (Vito et al. 2019; Nardini et al. 2019; Salvestrini et al. 2019) and archives (Evans et al. 2010; Menzel et al. 2016; Pâris et al. 2018; Webb et al. 2020), with the addition of a subsample of low-redshift quasars that present UV observations from the International Ultraviolet Explorer and X-ray data in archives. To obtain this quasar sample suitable for cosmological analyses, as many observational biases as possible have been meticulously inspected and removed (Risaliti & Lusso 2015; Lusso & Risaliti 2016; Risaliti & Lusso 2019; Salvestrini et al. 2019; Lusso et al. 2020). We note here some differences between our sample and the samples used in previous works. Here, we study this final sample of 2421 sources without any additional selection, such as the cut at redshift $z = 0.7$ previously used in some works (Lusso et al. 2020; Bargiacchi et al. 2022), to avoid any possible induced bias due to the reduction of the redshift sample (Dainotti et al. 2022a; Lenart et al. 2023).

2.1. Correction for the Redshift Evolution of the Luminosities

We clarify that previous works have not considered selection biases and redshift evolution with the exception of our works in the literature (Dainotti et al. 2022a; Bargiacchi et al. 2023; Lenart et al. 2023). Since quasars are high-redshift sources, we need to account for selection biases and redshift evolution effects. These factors could induce artificial correlations between the intrinsic physical quantities of the sources (Dainotti et al. 2013), such as the relation between the X-ray and UV luminosities for quasars. To correct for these effects, we have applied the statistical Efron & Petrosian method (Efron & Petrosian 1992), assuming that the luminosities evolve with redshift as $(1+z)^k$. This method has already been employed for GRBs (Dainotti et al. 2013, 2015, 2017, 2021a, 2023a) and quasars (Dainotti et al. 2022a; Lenart et al. 2023). The choice of a more complex function for redshift evolution would not affect the results (Singal et al. 2011; Dainotti et al. 2021c, 2022a). Thus, the de-evolved UV and X-ray luminosities are computed as $L'_{UV} = L_{UV}/(1+z)^{k_{UV}}$ and $L'_X = L_X/(1+z)^{k_X}$, respectively, by using L_{UV} and L_X obtained from the measured flux densities F_{UV} and F_X (in units of $\text{erg s}^{-1} \text{cm}^{-2} \text{Hz}^{-1}$) according to $L_{X,UV} = 4\pi d_l^2 F_{X,UV}$, where d_l is the luminosity distance in cm and the K -correction is assumed to be equal to 1 for quasars (Lusso et al. 2020). Here we consider a flat Λ CDM model. Our main gold quasar sample of 983 sources is obtained by fixing $\Omega_M = 0.3$ and $H_0 = 70 \text{ km s}^{-1} \text{Mpc}^{-1}$ in the distance luminosity. The values of k_{UV} and k_X used to determine L'_{UV} and L'_X are, respectively, $k_{UV} = 4.36 \pm 0.08$ and $k_X = 3.36 \pm 0.07$ (Dainotti et al. 2022a), which have been obtained within a flat Λ CDM model with $\Omega_M = 0.3$ and $H_0 = 70 \text{ km s}^{-1} \text{Mpc}^{-1}$, consistent with our assumption. The evolutionary parameter k depends on Ω_M , but not on H_0 (Dainotti et al. 2022a, 2023a; Lenart et al. 2023). Thus, when we change the value of Ω_M to

$\Omega_M = 0.1$ and $\Omega_M = 1$ to test the dependence of our results on the cosmological assumptions, we accordingly use the values of k_{UV} and k_X corresponding to these cosmologies. More precisely, these values are obtained from the functions $k_{UV}(\Omega_M)$ and $k_X(\Omega_M)$ reported in Dainotti et al. (2022a) and shown in their Figure 4. The resulting values are $k_{UV} = 4.79 \pm 0.08$ and $k_X = 3.81 \pm 0.06$ for $\Omega_M = 0.1$ and $k_{UV} = 3.89 \pm 0.08$ and $k_X = 2.88 \pm 0.06$ for $\Omega_M = 1$.

The choice of a specific Ω_M and thus, a value of k for the correction for evolution automatically induces the circularity problem. This issue can be completely overcome in the cosmological fit if we do not fix k a priori to compute the luminosities, but we apply the functions $k_{UV}(\Omega_M)$ and $k_X(\Omega_M)$ in the fitting procedure while leaving also the cosmological parameters free to vary, as already done in Lenart et al. (2023) for quasars and in Dainotti et al. (2023a) for GRBs. This allows us to avoid assuming a priori an underlying cosmology and to leave the evolutionary parameters free to vary together with the parameters of the fit. In our work, we also employ this circularity-free methodology when we fit Ω_M with the gold sample of 975 sources selected by applying the σ -clipping procedure to the relation between X-ray and UV fluxes, instead of luminosities. Indeed, the selection of the sample based on measured fluxes does not require any assumption on the cosmological model, contrary to the one based on luminosities, and, thus enables us to apply this circularity-free procedure to fit Ω_M with a sample that is not biased by any cosmological assumption.

2.2. Fitting Procedure

We have performed all fits with the Bayesian D'Agostini method (D'Agostini 2005). The likelihood function (\mathcal{L}) employed to constrain the parameters with quasars is given by Khadka & Ratra (2020a, 2020b), Lusso et al. (2020), Khadka & Ratra (2021), Colgáin et al. (2022a), Colgáin et al. (2022b), Khadka & Ratra (2022), Bargiacchi et al. (2022), and Lenart et al. (2023) as:

$$\ln \mathcal{L} = -\frac{1}{2} \sum_{i=1}^N \left[\frac{(y_i - \phi_i)^2}{s_i^2} + \ln(s_i^2) \right], \quad (1)$$

where “ln” is the natural logarithm and N is the number of sources. When we fit the luminosities, $y_i = \log_{10} L'_X$ of a quasar at redshift z_i , while ϕ_i is the logarithmic X-ray luminosity predicted from the fitted model. The quantity $s_i^2 = (\Delta \log_{10} L'_X)_i^2 + \gamma^2 (\Delta \log_{10} L'_{UV})_i^2 + \delta^2$ includes the statistical 1σ uncertainties (Δ) on both the luminosities and the intrinsic dispersion δ of the RL relation. The free parameters of the fit are γ , β , δ , and the ones of the cosmological model studied. The same methodology is applied when we fit fluxes instead of luminosities, just replacing $\log_{10} L'_{UV}$ and $\log_{10} L'_X$ with the measured $\log_{10} F_{UV}$ and $\log_{10} F_X$. In this case, γ_F and δ_F are the slope and the intrinsic dispersion of the linear relation.

2.3. σ -clipping Technique

Before applying the σ -clipping procedure, we have searched for possible outliers. Thus, we have computed the maximum values of $\Delta \log_{10} L'_{UV}/\log_{10} L'_{UV}$ and $\Delta \log_{10} L'_X/\log_{10} L'_X$. Points with large uncertainties on luminosities would not be removed by the σ -clipping and would have a higher weight in the cosmological fits compared to points with smaller

uncertainties. This check has revealed that our sample does not present any outliers of this kind. Independent of the Ω_M value, the maximum values of $\Delta \log_{10} L'_{UV}/\log_{10} L'_{UV}$ and $\Delta \log_{10} L'_X/\log_{10} L'_X$ are 0.022 and 0.013, respectively, with only one source with $\Delta \log_{10} L'_{UV}/\log_{10} L'_{UV} > 0.02$ and four sources with $\Delta \log_{10} L'_{UV}/\log_{10} L'_{UV} > 0.01$. Because these values are lower than $\sim 1\%$ – 2% , we do not remove any quasars from the initial sample. Hence, we apply the σ -clipping selection to all 2421 sources.

The σ -clipping allows us to reduce the intrinsic scatter of the RL relation by removing all sources with a vertical distance from the best-fit relation greater than a chosen threshold value by assuming a given cosmological model. It is used when dealing with relations presenting an intrinsic dispersion to remove possible outliers in the sample and assure a better determination of the free parameters of the relation. This procedure has already been successfully applied for quasars to constrain cosmological parameters (Lusso et al. 2020; Bargiacchi et al. 2021, 2022). We detail the method for our case. First, we fit the RL relation with the whole quasar sample assuming a flat Λ CDM model with $H_0 = 70 \text{ km s}^{-1} \text{ Mpc}^{-1}$ and $\Omega_M = 0.3$ or $\Omega_M = 0.1$ or $\Omega_M = 1$, to compute the X-ray and UV luminosities. The model used is the RL relation, thus ϕ_i of Equation (1) is $\phi_i = \gamma \log_{10} L'_{UV,i} + \beta$ for a source at redshift z_i . From this fit, we obtain the best-fit values of γ , β , and δ and their 1σ uncertainties. Then, we evaluate for each quasar at z_i the quantity:

$$\Sigma = \frac{|\log_{10} L'_{X,i} - (\gamma \log_{10} L'_{UV,i} + \beta)|}{\sqrt{\Delta^2 \log_{10} L'_{X,i} + \gamma^2 \Delta^2 \log_{10} L'_{UV,i} + \delta^2}} \quad (2)$$

, where we use the best-fit values previously obtained for γ , β , and δ . This quantity is exactly the one that is minimized in the fitting algorithm (i.e., the first term in square bracket of Equation (1)) to determine the parameters of the RL relation, and thus it is the most appropriate to estimate the discrepancy between the measured X-ray luminosity and the one predicted from the RL relation. Once we have computed Σ for each source, we select only quasars with $\Sigma \leq \sigma_{\text{clipping}}$ and we repeat the fit of the RL relation with this reduced sample. Since the fit to this new sample yields best-fit values of γ , β , and δ different from the ones of the previous fit, and thus different Σ values for each source, there will be quasars in the sample considered at this step that do not fulfill the requirement $\Sigma \leq \sigma_{\text{clipping}}$ anymore. Hence, we iterate this procedure until all sources in the selected sample verify the requisite. After this σ -clipping process, we obtain a final quasar sample, with the corresponding best-fit values and 1σ uncertainties of γ , β , and δ . We have chosen several σ_{clipping} values between 0.6 and 2 to investigate how the assumed σ_{clipping} , the best-fit value of δ , and the number of survived sources are related. This method selects the gold samples (983 quasars) within the flat Λ CDM model shown in the left panel of Figure 1 with its corresponding best-fit RL relation (purple line). We have also applied the same method to select the quasar samples using the observed fluxes instead of the luminosities. We fit the relation between $\log_{10} F_X$ and $\log_{10} F_{UV}$ for which γ_F , β_F , and δ_F are the slope, intercept, and intrinsic dispersion, respectively. The gold sample of 975 quasars obtained with the σ -clipping on fluxes is

shown in the left panel of Figure 4 with the best-fit linear relation (purple line).

2.4. Cosmological Fits

For each quasar sample produced by the σ -clipping with a specific threshold σ_{clipping} we have fitted a flat Λ CDM model. Following the fitting procedure described above, if we use the quasar sample selected through the σ -clipping on the luminosities corrected for a fixed redshift evolution, the quantities y_i and ϕ_i of Equation (1) for a source at z_i are, respectively, $y_i = \log_{10} F_{X,i} + \log_{10}(4\pi d_i^2(z_i)) - k_X \log_{10}(1+z_i)$ and $\phi_i = \gamma [\log_{10} F_{UV,i} + \log_{10}(4\pi d_i^2(z_i)) - k_{UV} \log_{10}(1+z_i)] + \beta$, where k_X and k_{UV} are the evolutions corresponding to the cosmological model assumed. Instead, if we perform the fit on the sample obtained from the σ -clipping on the measured fluxes, we require $y_i = \log_{10} F_{X,i} + \log_{10}(4\pi d_i^2(z_i)) - k_X(\Omega_M) \log_{10}(1+z_i)$ and $\phi_i = \gamma [\log_{10} F_{UV,i} + \log_{10}(4\pi d_i^2(z_i)) - k_{UV}(\Omega_M) \log_{10}(1+z_i)] + \beta$, thus avoiding the circularity problem. The luminosity distance d_i is computed fixing $H_0 = 70 \text{ km s}^{-1} \text{ Mpc}^{-1}$ and considering Ω_M as a free parameter with a wide uniform prior between 0 and 1. We also leave γ and β free to vary. Hence, we obtain the best-fit values of Ω_M , γ , β , and δ with their associated 1σ uncertainties.

3. Results

3.1. Golden Samples with an Assumed Cosmology

Our initial quasar sample is the most up-to-date for cosmological studies (Lusso et al. 2020) and composed of 2421 sources between $z = 0.009$ and $z = 7.54$. This sample is studied to define the gold quasar sample to obtain the tightest possible relation to be used as an efficient cosmological tool with the same precision achieved with SNe Ia. Differently from recent works (Lusso et al. 2020; Bargiacchi et al. 2021, 2022), we use the full sample of quasars at all redshifts and we correct for redshift evolution of the sample, as detailed before. So, we retain also sources at small redshifts which are excluded in most previous analyses. Different from Risaliti & Lusso (2019), the RL relation is already corrected for selection biases and redshift evolution as shown in Dainotti et al. (2022a) when the σ -clipping is applied. This procedure allows us to obtain the smallest intrinsic scatter of an already bias-free and evolution-free relation. Nevertheless, to constrain cosmological parameters, such as Ω_M , we are not only interested in reaching the smallest dispersion, but also in relying on a statistically sufficient number of sources. Thus, we need to find a compromise between these two antagonistic factors. Indeed, increasing the data set results in a larger intrinsic dispersion and vice versa. We divide our results in the search for two main golden samples, one assuming a given cosmological model and the second one without any cosmological assumption, thus completely overcoming the so-called circularity problem.

If we assume a flat Λ CDM model with $\Omega_M = 0.3$ and $H_0 = 70 \text{ km s}^{-1} \text{ Mpc}^{-1}$, the optimal number of sources is 983, obtained by requiring a threshold for the σ -clipping $\sigma_{\text{clipping}} = 1.788$, with a scatter $\delta = 0.007$ of the RL relation. The 983 quasars created in such a manner define the golden sample shown with the corresponding best-fit RL relation in the left panel of Figure 1.

Then, we use this sample to derive Ω_M with the Markov Chain Monte Carlo (MCMC) computation and leaving contemporaneously free the values of Ω_M in the range from 0

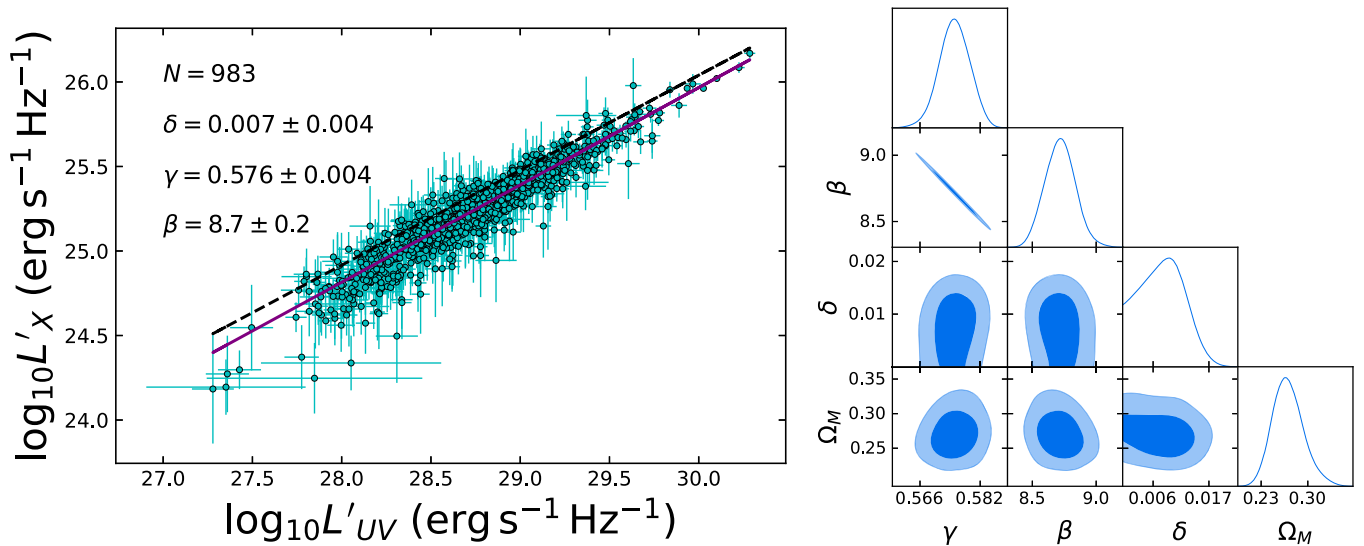


Figure 1. Left panel: the golden sample of 983 quasars obtained with the σ -clipping on the L_X-L_{UV} relation assuming a flat Λ CDM model with $\Omega_M = 0.3$ and $H_0 = 70 \text{ km s}^{-1} \text{ Mpc}^{-1}$. The resulting best-fit values of the parameters are the slope $\gamma = 0.576 \pm 0.004$, the normalization $\beta = 8.7 \pm 0.2$, and the dispersion $\delta = 0.007 \pm 0.004$. Blue points are the sources with error bars representing the statistical 1σ uncertainties and the best-fit linear relation is drawn as a purple line. The black dashed line is the best-fit line for the 2036 quasars used in Lusso et al. (2020), for which $\gamma = 0.562 \pm 0.011$, $\beta = 9.2 \pm 0.3$, and $\delta = 0.221 \pm 0.004$ after correction for evolution. Right panel: cosmological results in a flat Λ CDM model from our golden sample shown in the left panel. This shows the values of Ω_M , γ , β , and δ . The contour levels at 68% and 95% are represented by the inner dark and light blue regions, respectively.

to 1 using a uniform distribution and the parameters of the RL relation, γ (the slope), β (the normalization), and δ (the dispersion). We fix $H_0 = 70 \text{ km s}^{-1} \text{ Mpc}^{-1}$ assuming a standard flat Λ CDM model. The results of this analysis are shown in the right panel of Figure 1 where the corner plot of the RL relation parameters and Ω_M are obtained when we perform the correction for redshift evolution. The best-fit value yields $\Omega_M = 0.268 \pm 0.022$, which carries the same uncertainty on Ω_M found with the Pantheon sample (1048 SNe Ia) assuming the same cosmology (Scolnic et al. 2018), as shown with the horizontal blue line in Figure 2. We also recover the Ω_M we have assumed to build this sample within 0.68σ .

To assess to what extent the number of sources impacts the values and the uncertainty on Ω_M , we show in the upper panel of Figure 2 the value of σ_{Ω_M} versus the number of sources and varying of the σ -clipping shown as a color bar. In the upper panel of Figure 2, we start from the total sample of sources and we apply a very restrictive criterion for the σ -clipping = 0.6 and then we continue with larger values of σ -clipping until arriving at 2.0. When we change the values of the σ -clipping, the smaller the σ -clipping, the smaller the sample size obtained if we consider sources from 300 to 1000 and from 1700 to 2000; but when the σ -clipping is too small (0.045 for example, see the red point in the upper panel of Figure 2), then the uncertainty on Ω_M becomes larger. Since the σ -clipping and the number of sources also determine the intrinsic dispersion of the RL relation, thus we show in the bottom panel of Figure 2 the intrinsic scatter as a function of the number of sources and of the σ -clipping shown as a color bar. It is clear from this figure that the dispersion of the RL relation increases monotonically with an increase of the sample size, starting from around 1000 sources, while to achieve smaller dispersion the trend is rather flat from 300 to 1000 sources. This increasing trend of the dispersion of RL relation as a function of the number of sources is reflected by the increasing value of the uncertainty on Ω_M in the range between 1000 and 1300. However, the highly nonlinear process of obtaining cosmological parameters, in this

case the value of σ_{Ω_M} , and the cut that the σ -clipping induces in the initial sample does not allow a straightforward comparison between the upper and lower panels of Figure 2. To conclude, the number of 975 sources is the optimal compromise to obtain the smallest uncertainty on Ω_M taking into consideration the dispersion. Indeed, if we still would enlarge further the σ -clipping the number of sources would become larger together with the dispersion of the RL relation. This is the reason why we have mentioned before the relevance to reach a compromise among the number of sources used and the dispersion of the RL relation and consequently the uncertainty on Ω_M before the increase we observe between 1000 and 1700 sources. We stress that the subsamples shown in Figure 2 are not subsamples of the gold sample, but they are samples drawn independently, however, with the same procedure of the σ -clipping starting from the full sample assuming a flat Λ CDM model. Continuing on the evaluation of how many number of sources are needed to obtain the most probable value of Ω_M we show a color map in the upper panel of Figure 3 where the probability density function (PDF) of Ω_M is plotted as a function of the number of sources. We note from this figure that 983 sources are the best sample as it provides closed cosmological contours with the highest corresponding probability. To complement this information, we also plotted in the bottom panel of Figure 3 the Ω_M value as a function of σ -clipping and as a function of the probability density for Ω_M shown in the color bar. From this figure it is clear that a σ -clipping of 1.8 is the optimal value to choose our gold sample since the scatter on Ω_M becomes small enough to reach the precision of the SN Ia Pantheon sample. To check this result against the cosmological settings, we also test the assumptions of $\Omega_M = 1$ (universe filled by matter in which $\Lambda = 0$), and $\Omega_M = 0.10$ (very close to the De Sitter universe). We obtain that the best-fit values of Ω_M are consistent within less than 3σ with the a priori assumption. In fact, when we choose the golden sample of 980 quasars derived with the $\sigma_{\text{clipping}} = 1.788$ assuming $\Omega_M = 0.10$, we obtain $\Omega_M = 0.083 \pm 0.009$, while when we select the sample of 968

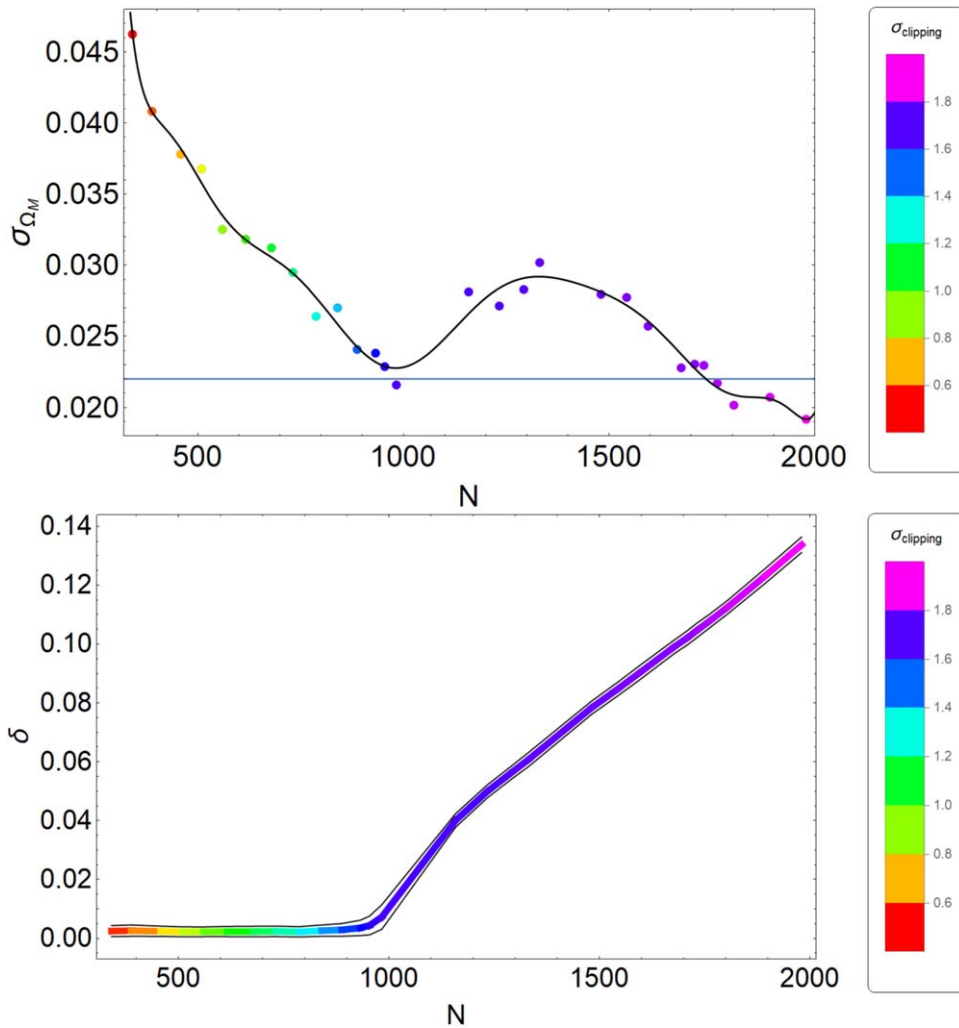


Figure 2. Upper panel: the uncertainty of Ω_M as a function of the number of sources and as a function of the σ -clipping shown with the color bar on the right. The solid black line shows the best fit of the decreasing trend of the uncertainty on Ω_M vs. the number of sources, while the horizontal blue line denotes the uncertainty on Ω_M reached with the Pantheon SNe Ia sample. This is obtained for our golden sample under the assumption of a flat Λ CDM model with $\Omega_M = 0.3$ and $H_0 = 70 \text{ km s}^{-1} \text{ Mpc}^{-1}$. Lower panel: the intrinsic dispersion of the RL relation as a function of the number of sources and as a function of the σ -clipping indicated on the right as a color bar. Black lines mark the 1σ uncertainty on the δ values.

quasars assuming $\Omega_M = 1$, we obtain $\Omega_M = 0.910 \pm 0.055$ for $\sigma_{\text{clipping}} = 1.785$.

3.2. The Anderson–Darling Test for Different Gold Samples and the Parent Population

To check the similarity between the gold sample and the parent population, we have applied the Anderson–Darling test to compare both the flux–flux distribution and the luminosity–luminosity distribution from the parent population and the gold sample. The results of the test show that the luminosities and fluxes of the gold sample are not compatible both in X-rays and UV with the parent population. In addition, the sample from the parent population used by Lusso et al. (2020) also is not compatible with our gold sample. It is not surprising that we can have different results when other probes are added to quasars since probes with smaller uncertainties (s in Equation (1)) weigh more than the ones with larger uncertainties, being the s values in the denominator of the likelihood function. In addition, since our gold sample is already a sample for which the selection biases have been removed, the cosmological results from this sample should not

necessarily be the same as the enlarged sample (the parent population) if the parent population undergoes selection biases and redshift evolution. Indeed, the results of the cosmological parameters may change if evolutionary effects are not considered (Dainotti et al. 2013, 2022b, 2023b; Lenart et al. 2023). In relation instead of our gold sample both in X-rays and UV derived from a given cosmology ($\Omega_M = 0.3$ and $H_0 = 70 \text{ km s}^{-1} \text{ Mpc}^{-1}$) these are compatible with the gold sample that originated assuming other cosmologies ($\Omega_M = 0.1$ and $H_0 = 70 \text{ km s}^{-1} \text{ Mpc}^{-1}$, and $\Omega_M = 1$ and $H_0 = 70 \text{ km s}^{-1} \text{ Mpc}^{-1}$). This ensures that the selection of our Gold sample does not depend on cosmological models.

3.3. A Circularity-free Golden Sample

To guarantee further that we completely avoid the circularity problem for the choice of the golden sample of quasars, we use the $F_X - F_{\text{UV}}$ relation, the observer-frame relation corresponding to the RL relation. As previously, we apply the same σ_{clipping} procedure to reduce the scatter of the $F_X - F_{\text{UV}}$ relation. A $\sigma_{\text{clipping}} = 1.78$ identifies an optimal sample of 975 sources, shown in the left panel of Figure 4. We then use this sample

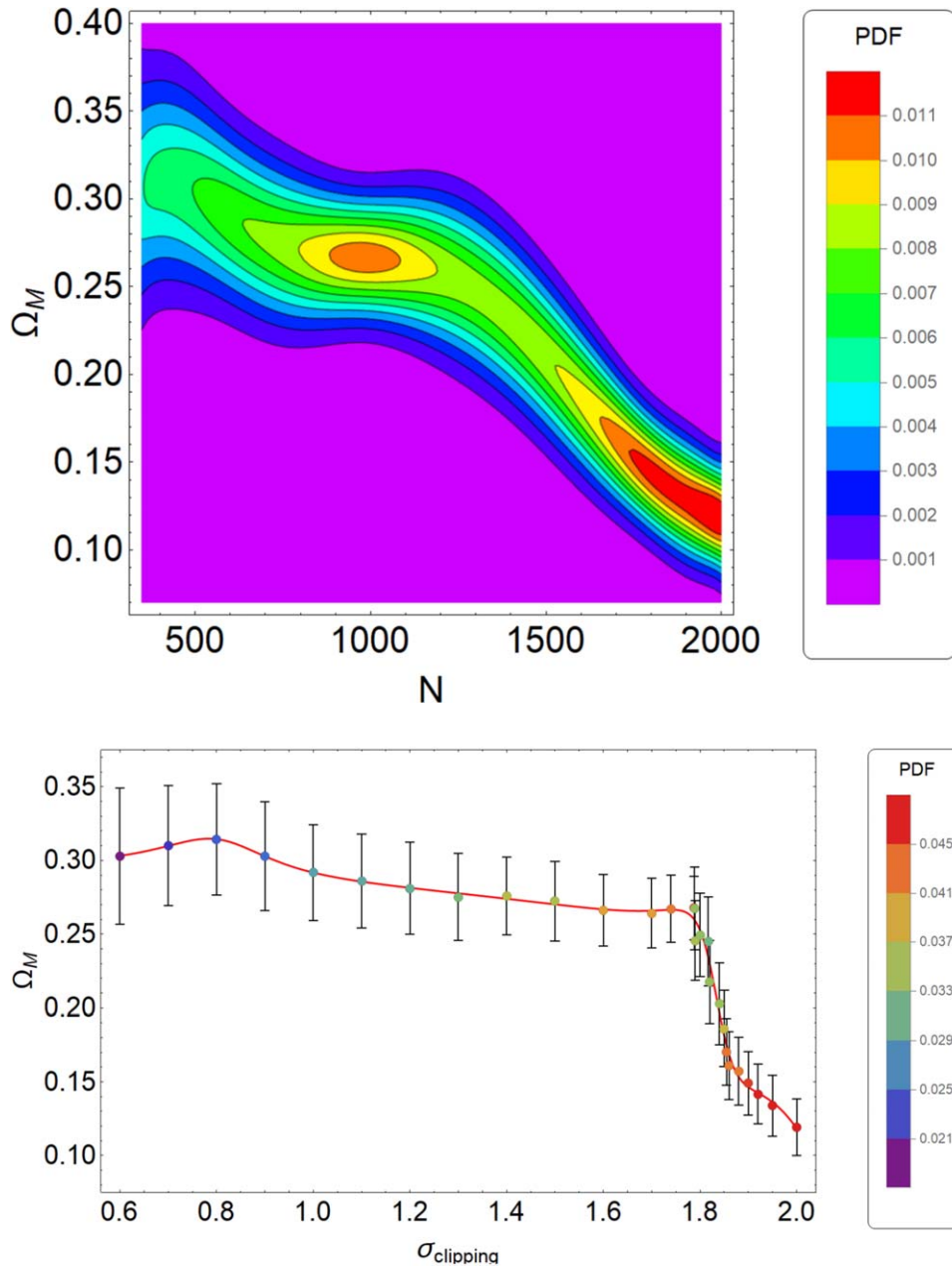


Figure 3. Upper panel: the value of Ω_M and its associated uncertainty vs. the number of quasars. The color bar on the right shows the normalized probability density, indicating for each sample size the most probable value of Ω_M , and thus the smallest uncertainty on Ω_M . This figure indicates that the smallest error bar on Ω_M (the red contour) is achieved for $N \approx 2000$, which yields $\Omega_M = 0.119 \pm 0.019$. This is obtained for our golden sample assuming a flat Λ CDM model. Bottom panel: value of Ω_M with its corresponding 1σ uncertainty as a function of the σ -clipping threshold, and a PDF is shown with the color bar on the right side. The red line is the best fit to the Ω_M points.

(free from any circularity problem) to derive Ω_M and the RL parameters (see the 2 section), and we obtain $\Omega_M = 0.107 \pm 0.047$, as reported in the right panel of Figure 4.

Additionally, to assure that our findings are not driven by low- z quasars ($z < 0.7$), which according to Lusso et al. (2020) could be affected by host galaxy contamination and lower data quality, we have removed these sources (47 quasars) from the golden sample, obtaining $\Omega_M = 0.125 \pm 0.040$.

4. MCMC Sampling Uncertainty

To guarantee further that our results are not due to the use of a single run in the MCMC calculation and that the sampling procedure is stable, we show the results of the computation

when it is run 100 times. With this procedure, we obtain $\langle \Omega_M \rangle = 0.112 \pm 0.048$, where the symbol $\langle \rangle$ denotes the average value. We have investigated the reliability of the best-fit value and 1σ uncertainty on Ω_M obtained in each of the cosmological fits. Our results are derived by fitting the free parameters of the models studied with only one MCMC run. We test these results against the sampling errors on the parameters derived in the sampling procedure. To this end, we have looped all the MCMC samplings 100 times for each model, then computing the mean value of Ω_M and its uncertainty. The results obtained with this method for both quantities and all the cosmological cases investigated in our analysis are shown in Table 1. These results are completely

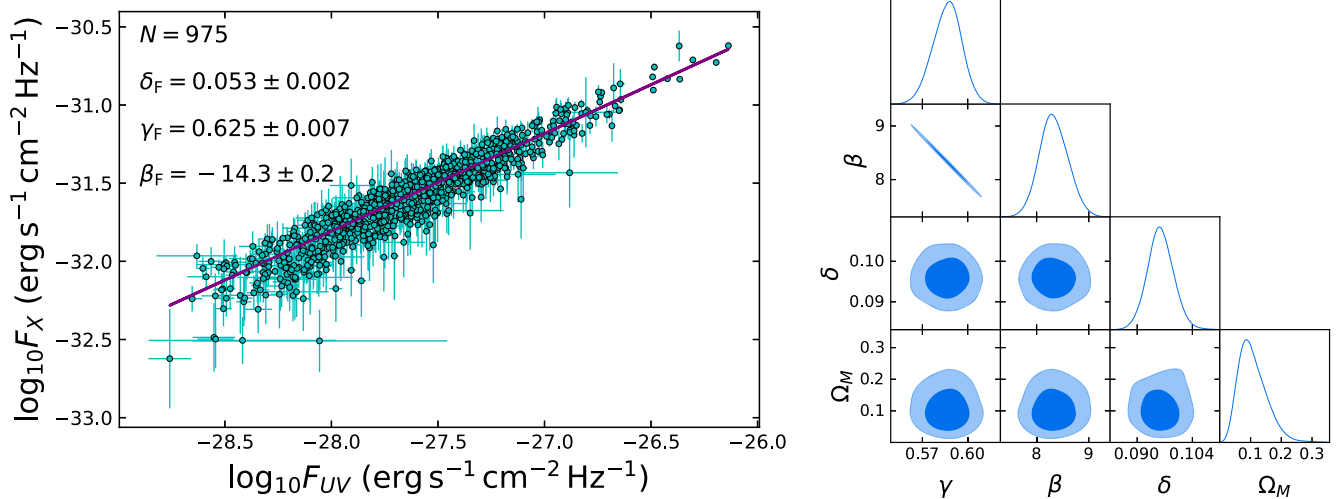


Figure 4. Left panel: the gold sample of 975 quasars generated with the σ -clipping on the F_X-F_{UV} relation with the best-fit parameters being $\gamma_F = 0.625 \pm 0.007$, $\beta_F = -14.3 \pm 0.2$, and $\delta_F = 0.053 \pm 0.002$. Blue points are the sources with error bars representing the statistical 1σ uncertainties and the best-fit linear relation is drawn as a purple line. Right panel: cosmological results from the golden sample shown in the left panel. This corner plot shows the values of Ω_M , γ , β , and δ . The contour levels at 68% and 95% are represented by the inner dark and light blue regions, respectively.

consistent with the ones obtained from only one run of the MCMC, with a maximum discrepancy of 0.08σ .

5. Discussion and Conclusions

In the choice of the golden samples with a fixed cosmology we have first assumed a flat Λ CDM model with $\Omega_M = 0.3$ and $H_0 = 70 \text{ km s}^{-1} \text{ Mpc}^{-1}$. This is a necessary starting cosmological model and value for Ω_M , because our aim is to compare the results of our uncertainties with the ones obtained using the Pantheon sample for the same cosmological model. Regarding the sample size, we note that the 1048 Pantheon SNe Ia have been slimmed down from an original sample of 3473 events, with a cutting of 70% of the starting data set (Scolnic et al. 2018). Instead, in our work, we reduce the initial sample of 2421 quasars by $\sim 60\%$ to build all the golden samples studied. Thus, the slimming of our sample is even less severe than the one of SNe Ia. We here compare the SN Ia and quasar samples from a mere statistical point of view and, not for the purpose to compare them from a physical and an observational point of view, since they differ on both aspects.

Our results highlight that the uncertainty on Ω_M depends on the assumed cosmology, namely the smaller the uncertainty the more we are closer to the most likely value of the cosmological parameter. The uncertainty on Ω_M assuming $\Omega_M = 0.10$ is 6.7 times smaller than the one in the case of $\Omega_M = 1$. With the evolutionary parameters included and with no information about the underlying cosmology, we still obtain a value of Ω_M compatible with the De Sitter universe at the 2.3σ level, and is not compatible with the current value of $\Omega_M = 0.338 \pm 0.018$ found in Brout et al. (2022) at the level of 4.58σ . We here clarify that this estimate on Ω_M found by us is larger (more than 1σ) than the observed baryonic matter today if we consider the value found by Planck measurements of the CMB (Planck Collaboration et al. 2020), which is 0.0500 ± 0.0002 . Although the value of the uncertainty in the gold sample identified by the F_X-F_{UV} relation is 2.14 times larger than the one obtained by the Pantheon sample of SNe Ia (Scolnic et al. 2018), we can still obtain an uncertainty comparable with the 740 SNe Ia shown in Betoule et al. (2014) where $\sigma_{\Omega_M} = 0.042$.

Table 1
The Results of the Looped Computations for 100 Iterations

σ_{clipping}	$\Omega_{M,\text{start}}$	$\langle \Omega_M \rangle$	$S_{<\Omega_M>}$	$\langle \sigma_{\Omega_M} \rangle$	$S_{<\sigma_{\Omega_M}>}$
Luminosities					
1.788	0.3	0.2681	0.0010	0.0223	0.0007
1.788	0.1	0.0836	0.0004	0.0086	0.0004
1.785	1	0.9141	0.0024	0.0536	0.0013
Fluxes					
1.78	...	0.1124	0.0021	0.0475	0.0021

Note. S denotes the standard deviation of a given parameter and $\Omega_{M,\text{start}}$ is the value of Ω_M assumed to obtain the corresponding golden sample with the threshold value σ_{clipping} . The cases in which the σ -clipping is applied to the relation in luminosities or in fluxes are also shown separately.

The result on Ω_M obtained with the golden sample of 975 quasars from the F_X-F_{UV} relation (i.e., $\Omega_M = 0.107 \pm 0.047$) is compatible with $\Omega_M = 0.125 \pm 0.040$ derived from the same golden sample to which we have removed low- z sources due to the contamination of the host galaxies (47 quasars). However, when a larger sample is available is necessary to check if the current results still hold within 1σ . Although there have been several studies that have measured Ω_M with quasars with lower precision (e.g., Khadka & Ratra 2020b; Colgáin et al. 2022a; Khadka & Ratra 2022), we here for the first time obtain a value with a higher precision with QSOs alone, which is not due to a circular argument, since it is based on a flux-flux relation. In addition, the analysis performed by us using the luminosities and assuming a given cosmological model is meant to show the great potentiality of quasars to be used as standardizable candles even currently when an appropriate sample size and reduced uncertainties is used. Indeed, the analysis we have shown here is similar to the analysis we performed in Dainotti et al. (2023a) where we were not interested in knowing the value of the cosmological parameters, but we were focused on how many sources, in this case quasars, are needed to reach the same precision of the SN Ia Pantheon sample.

In conclusion, we have shown that quasars alone with the RL relation can now be upgraded to reliable standard candles to measure cosmological parameters such as Ω_M with the same precision as SNe Ia, but at higher redshifts, up to 7.5, when a golden sample of quasars is chosen.

We thank Beta Lusso and Risaliti Guido for discussions on the role of selection biases in the sample and Biagio De Simone for help running a couple of notebooks for the MCMC sampling.

ORCID iDs

M. G. Dainotti  <https://orcid.org/0000-0003-4442-8546>
 G. Bargiacchi  <https://orcid.org/0000-0002-0167-8935>
 A. Ł. Lenart  <https://orcid.org/0000-0003-1943-010X>
 S. Nagataki  <https://orcid.org/0000-0002-7025-284X>
 S. Capozziello  <https://orcid.org/0000-0003-4886-2024>

References

- Alam, S., Aubert, M., Avila, S., et al. 2021, *PhRvD*, **103**, 083533
 Bañados, E., Venemans, B. P., Mazzucchelli, C., et al. 2018, *Natur*, **553**, 473
 Bargiacchi, G., Benetti, M., Capozziello, S., et al. 2022, *MNRAS*, **515**, 1795
 Bargiacchi, G., Dainotti, M. G., Nagataki, S., & Capozziello, S. 2023, *MNRAS*, **521**, 3909
 Bargiacchi, G., Risaliti, G., Benetti, M., et al. 2021, *A&A*, **649**, A65
 Betoule, M., Kessler, R., Guy, J., et al. 2014, *A&A*, **568**, A22
 Brout, D., Scolnic, D., Popovic, B., et al. 2022, *ApJ*, **938**, 110
 Colgáin, E. Ó, Sheikh-Jabbari, M. M., Solomon, R., et al. 2022a, arXiv:2203.10558
 Colgáin, E. Ó, Sheikh-Jabbari, M. M., Solomon, R., Dainotti, M. G., & Stojkovic, D. 2022b, arXiv:2206.11447
 D'Agostini, G. 2005, arXiv:physics/0511182
 Dainotti, M., Lenart, A., Sarracino, G., et al. 2020, *ApJ*, **904**, 19
 Dainotti, M., Levine, D., Fraija, N., & Chandra, P. 2021a, *Galax*, **9**, 95
 Dainotti, M., Petrosian, V., Willingale, R., et al. 2015, *MNRAS*, **451**, 3898
 Dainotti, M. G., Bargiacchi, G., Lenart, A. Ł., et al. 2022a, *ApJ*, **931**, 106
 Dainotti, M. G., Cardone, V. F., Piedipalumbo, E., & Capozziello, S. 2013, *MNRAS*, **436**, 82
 Dainotti, M. G., Lenart, A. Ł., Chraya, A., et al. 2023a, *MNRAS*, **518**, 2201
 Dainotti, M. G., Lenart, A. Ł., Fraija, N., et al. 2021b, *PASJ*, **73**, 970
 Dainotti, M. G., Lenart, A. Ł., Chraya, A., et al. 2023b, *MNRAS*, **518**, 2201
 Dainotti, M. G., Nagataki, S., Maeda, K., Postnikov, S., & Pian, E. 2017, *A&A*, **600**, A98
 Dainotti, M. G., Nielson, V., Sarracino, G., et al. 2022b, *MNRAS*, **514**, 1828
 Dainotti, M. G., Petrosian, V., & Bowden, L. 2021c, *ApJL*, **914**, L40
 Dainotti, M. G., Postnikov, S., Hernandez, X., & Ostrowski, M. 2016, *ApJL*, **825**, L20
 Dainotti, M. G., Sarracino, G., & Capozziello, S. 2022c, *PASJ*, **74**, 1095
 Dainotti, M. G., Willingale, R., Capozziello, S., Fabrizio Cardone, V., & Ostrowski, M. 2010, *ApJL*, **722**, L215
 Dainotti, M. G., Young, S., Li, L., et al. 2022d, *ApJS*, **261**, 25
 Efron, B., & Petrosian, V. 1992, *ApJ*, **399**, 345
 Evans, I. N., Primini, F. A., Glotfelty, K. J., et al. 2010, *ApJS*, **189**, 37
 Khadka, N., & Ratra, B. 2020a, *MNRAS*, **492**, 4456
 Khadka, N., & Ratra, B. 2020b, *MNRAS*, **497**, 263
 Khadka, N., & Ratra, B. 2021, *MNRAS*, **502**, 6140
 Khadka, N., & Ratra, B. 2022, *MNRAS*, **510**, 2753
 Khadka, N., Zajaček, M., Prince, R., et al. 2023, *MNRAS*, **522**, 1247
 Lenart, A. Ł., Bargiacchi, G., Dainotti, M. G., Nagataki, S., & Capozziello, S. 2023, *ApJS*, **264**, 46
 Lusso, E., & Risaliti, G. 2016, *ApJ*, **819**, 154
 Lusso, E., Risaliti, G., Nardini, E., et al. 2020, *A&A*, **642**, A150
 Menzel, M. L., Merloni, A., & Georgakakis, A. 2016, *MNRAS*, **457**, 110
 Nardini, E., Lusso, E., Risaliti, G., et al. 2019, *A&A*, **632**, A109
 Pâris, I., Petitjean, P., Aubourg, É., et al. 2018, *A&A*, **613**, A51
 Perlmutter, S., Aldering, G., Goldhaber, G., et al. 1999, *ApJ*, **517**, 565
 Planck Collaboration, Aghanim, N., Akrami, Y., et al. 2020, *A&A*, **641**, A6
 Riess, A. G., Filippenko, A. V., Challis, P., et al. 1998, *AJ*, **116**, 1009
 Risaliti, G., & Lusso, E. 2015, *ApJ*, **815**, 33
 Risaliti, G., & Lusso, E. 2019, *NatAs*, **3**, 272
 Rodney, S. A., Riess, A. G., Scolnic, D. M., et al. 2015, *AJ*, **150**, 156
 Salvestrini, F., Risaliti, G., Bisogni, S., Lusso, E., & Vignali, C. 2019, *A&A*, **631**, A120
 Scolnic, D. M., Jones, D. O., Rest, A., et al. 2018, *ApJ*, **859**, 101
 Singal, J., Petrosian, V., Lawrence, A., & Stawarz, Ł. 2011, *ApJ*, **743**, 104
 Vito, F., Brandt, W. N., Bauer, F. E., et al. 2019, *A&A*, **630**, A118
 Webb, N. A., Coriat, M., Traulsen, I., et al. 2020, *A&A*, **641**, A136
 Yonetoku, D., Murakami, T., Nakamura, T., et al. 2004, *ApJ*, **609**, 935